Nat. Hazards Earth Syst. Sci. Discuss., 3, 2537–2564, 2015
www.nat-hazards-earth-syst-sci-discuss.net/3/2537/2015/
doi:10.5194/nhessd-3-2537-2015

Natural Hazards and Earth System Sciences
Discussions
Open Access

Movement of the Donglingxin landslide, China, induced by reservoir inundation and rainfall

J. Yu[1,2], R. B. Wang[1,2], W. Y. Xu[1,2], L. Yan[1,2], J. C. Zhang[1,2], and Q. X. Meng[1,2]

[1]Research Institute of Geotechnical Engineering, Hohai University, Nanjing, China
[2]Key Laboratory of the Ministry of Education for Geomechanics and Embankment Engineering, Hohai University, Nanjing, China

Received: 22 March 2015 – Accepted: 31 March 2015 – Published: 15 April 2015

Correspondence to: R. B. Wang (rbwang_hhu@foxmail.com)

Published by Copernicus Publications on behalf of the European Geosciences Union.

Abstract

With numerous high mountains, deep valleys and turbulent rivers, many hydropower plants have been constructed in the south-west China. Reservoir bank slopes are very common in this area, these slopes are widespread and quite often involved in deformation that can result in serious damage and casualties. In case of the Donglingxin landslide, for an in-depth study of processes that can trigger these events, the deformation characteristics and the failure mechanisms of the slope were performed on a detail scale, based on an intensive monitoring of rainfall events, reservoir level fluctuation and groundwater movement. The deformation of the upper part of slope is mainly induced by rainfall events, reservoir level fluctuation affects the deformation of the lower part of slope. The increase of pore water pressure may result in the failure of slope. The filed investigation suggest that the slope is unstable. Drainages is the only stabilization measure which can be implemented, due to very complex geological and geomorphology condition.

1 Introduction

In recent years, a large number hydropower plants have been constructed in south-west China, and many landslides are reactivated by initial impoundment of the reservoirs, so instabilities of reservoir bank slopes have been a challenging issue for hydropower projects. Many failure events of reservoir bank slope have been reported in China (Huang, 2009). In 1961, a reservoir-induced landslide near the Zhaxi dam claimed the lives of over 70 workers (Jin and Wang, 1988). In 2003, the Qianjiangping landslide killed 24 people and destroyed 346 houses (Wang et al., 2004). The landslide-related direct and indirect economic losses in China costs more than 20 billion Yuan every year (Bai et al., 2014).

Researchers in China studying the deformation characteristics and triggering mechanisms of landslides (Qi, 2006) found that reservoir level fluctuation and rainfall cause

NHESSD
3, 2537–2564, 2015

deformation leading to landslides (Wang et al., 2008).Infiltration of rainfall accelerates the deformation of the landslide and deteriorates its stability (Wang et al., 2012).

Sanbanxi procject is located on the lower reach of the Qingshui River (Fig. 1), the main stream of the Yuanjiang River. It is the sole hydropower plants with multi-year regulating ability on the Yuanjiang river. It has a concrete face rockfill dam with maximum dam height of 185.5 m and a total installed capacity of 1000 MW (4 × 250 MW). The reservoir has a normal pool level 475 m and a total capacity of 3.75 billion m^3. The total area of the reservoir is 79.56 km^3, and the backwater of the reservoir is 120 km long. The Donglingxin landslide is located on the south bank of the Qingshui River, southeast of Liuchuan, Jianhe Country, Guizhou Province. It's is 80 km upstream of the Sanbanxi dam (Fig. 1), on which there is a village of dozens of inhabitants. With a volume of 20.7 million m^3, it is the largest ancient slide in the reservoir. The slide was reactivated by the first impoundment of the reservoir in July 2007. Due to the narrow valley at the slide location, the supports and protections measure is difficult to be used. The Liuchuan town in the immediate vicinity will be destroyed, once the slide fails. Therefore, the study of its deformation characteristics and the failure mechanisms is significant for assuring the safety of reservoir and dam.

In this paper, we discuss the deformation characteristics and triggering mechanism of the Donglingxin landslide through geological investigation and comprehensive analysis of the 2 year observation data. The deformation tendency was also assessed.

2 Description of the Donglingxin landslide

The Donglingxin landslide is a reservoir bank slope, its natural slope surface mainly tends toward N 35° W. There are two gullies on the edge of landslide. Geological survey indicated that the Donglingxin landslide is a large-scale ancient landslide, which is an accumulation of several consequent slides along the bank slope, several secondary slumps occurred in its front, most of the landslide area is underlain by coarse silty clay and stone, relaxed and broken rock mass was found only at the foot of the excavation slope and the central ridge. The landslide can be divided into two zones, Fig. 2 shows the topography and zoning of the Donglingxin landslide (Google earth), (i) zone 1 extends along the Qingshui River with approximately 280 m in height and 310 km^2 in area, it is 800 m wide and lies between the riverbed and elevation 700 m, and the landform looks like a round-backed armchair (ii) zone 2 is located in the upper southern region of zone 1 with 120–220 m in height and 68 km^2 in area it is 200 m wide and lies between elevation 600 and 825 m. Borehole data indicate that the landslide is generally between 18 and 96 m thick, the thickest being about 140 m. The landslide volume is about 20 million m^3. The slope of zone 1 ranges from 22° in the upper part to 40° in the lower part. The slope of zone 2 ranges from 17 to 35°. Houses are built at elevations of 670–702 m. Figure 3 shows the local village and rice paddies at an elevation of 692 m.

The landslide is located in a sub-humid subtropical climate zone with a mean annual precipitation of 1280.5 mm. Most of precipitation occurs in the months from April to August with a maxmum daily precipitation up to 133.3 mm. The lowest water level of the Sanbanxi Reservoir is about 425 m, while the highest water level of the reservoir after inundation is 472 m. Groundwater in slope is pore phreatic in Quaternary and bedrock fissure water. The precipitation recharges groundwater within the landslide. There are two drainage paths: (1) through fracture network downwards into the underlying bedrock, (2) discharge into the gully directly.

3 Landslide geology

The stratum outcropped in this region are Banxi group of Algonkian system and Quaternary. The lithology at the landslide is illustrated in three profiles presented in Fig. 5 along the sections marked by I-I′, II-II′, and III-III′ in Fig. 4. Stratigraphic geo-materials differ in compositions and characteristics as described in detail below.

1. Member 1 of Qingshui formation of Banxi Group of Algonkian system (P^1_{tbq}): mainly consisting of blastobedding tuffaceous sandstone, tuffaceous silty slate and blastobedding tuff.

2. Quaternary, including eluvium and diluvium (Q_4^{edl}), accumulated layer landslide (Q_4^{del}) and human accumulation layer (Q_4^{s})

   Eluvium and diluvium (Q_4^{edl}) is comprised of silt clay, with mixture of broken stones, it is found in the slope mostly behind the village and on both sides of the ridge with thickness of 1–5 m.

   Accumulated layer landslide (Q_4^{del}) is composed of four types of geological materials. It is 18–96 m thick. The stratigraphic physical and mechanical properties are given in Table 1 (provided by HydroChina Zhongnan Engineering).

   i. Coarse-grained silty clay with mixture of strongly weathered broken stones are distributed on the surface of the landslide except at the lower part of zone 1 and east of zone 2. The content rate of rock is 20–40 %. The thickness is generally 5–12 m with some places at the upper part of the deposit over 20 m thick.

   ii. Strongly weathered broken stones and gravel with mixture of silty clay was observed in the middle of the landslide, and covered with layer i. The content rate of rock in this strata is high. The thickness of this strata varies greatly, from 6.3–12 m in the west and north to 51.2–79.1 m in the central and southern parts of the landslide.

   iii. Cataclastic rock mass comprised of blastobedding tuffaceous sandstone, tuffaceous silty slate and blastobedding tuff, is distributed mainly at the lower part of the landslide. This strata has moderate or strong weathering, with good rock mass integrity. The thickness is over 120 m.

   iv. The sliding zone mainly consists of yellow brown and dust color silty clay with thickness of 1.3–11.3 m, a small amount of gravel distributed in the front.

NHESSD
3, 2537–2564, 2015

Human accumulation layer (Q_4^s) is gravel, about 5 m thick, laid during the highway excavations.

4 Deformation features and stabilization measures

4.1 Deformation features

The first impoundment of the Sanbanxi reservoir began in January 2006. At the end of July 2007 the reservoir level reached 472, 3 m below the normal storage level. Field investigations showed that cracks appeared at the concrete foundation of house (Fig. 6) and the west boundary of zone 1 at elevations of 665–700 m where the head of gully at the end of July 2007. The deformation tendency of the surface of landslide aggravated in 2008. This newly developed deformation is described below.

1. In the eastern gully, where the landslide is covered by quaternary overburden, a few cracks 1–5 cm wide and about 2 m long were observed along N 10° W–N 20° E.
2. In the rice paddies at elevation 692 m, along N 10° W–N 5° E, a tension crack was observed; it was 15–20 cm wide, more than 2 m long, and 10–30 cm in visible depth (Fig. 6).
3. The landslide experienced prolonged periods of intense rainfall, muddy water was observed coming out of the toe of zone 1 (Fig. 7).

The field investigation suggested that there are two sliding surface in the slope (Fig. 5). One is shallow located within the lower accumulated layer landslide, which has a rotational slide mode. The other is deep through the sliding zone. It is a translational slide, and the slope may appear bedding landslide. The deformation characteristics show: the landslide belongs to thrust load caused landslide, the landform and material buildup is geological condition of landslide, abundant rainfall and reservoir fluctuation are primary induction factors of landslide.

4.2 Stabilization measures

Due to the narrow valley at the landslide location, the supports and protections measure is difficult to be used. Many researches (Fleming et al., 1989; Iverson et al., 1997) suggested that, the increase of pore water pressure caused the decrease of shear strength, therefore, drainage is only stabilization measure which can be used.

Figure 8 shows a drainage tunnel at 500 m elevation, excavated through the bottom of the landslide. To reduce the saturation level at the sliding zone and increase landslide stability, drainage holes were drilled in the tunnel for draining the groundwater around the sliding zone, and the bedrock fissure water. The drainage tunnel construction began in March 2010. Figure 9a shows the drainage tunnel under construction, and the water draining out of the tunnel wall can be seen in Fig. 9b. The main tunnel was completed in May 2011.

4.3 Monitoring system

A large number of monitoring instruments were installed to enable real-time recording of the slope deformation and analysis of the deformation tendencies. Two monitoring methods – geodetic detection and borehole monitoring – were used to establish the vectors of the dome displacements and to measure the groundwater level of the slope, respectively.

For geodetic detection, three horizontal displacement datum points and three vertical displacement datum points made of concrete were constructed, as well as nine observation points at the surface of the slope (Fig. 8). In October 2009, observation data of the slope deformation were obtained. Additionally, eight boreholes were drilled for measuring groundwater level.

NHESSD
3, 2537–2564, 2015

5 Monitoring results and analysis

5.1 Groundwater

The data of groundwater level from the eight boreholes and the reservoir, rainfall data are plotted in Fig. 10. Looking at the groundwater level of boreholes ZK11 and ZK14 located in the lower part of landslide, four fluctuations can be identified.

1. From November 2009 to February 2010 the groundwater level at ZK11 and ZK14 dropped from 452.32 and 475.83 to 428.19 and 455.70 m, respectively. In this period, rainfall was low and the reservoir drainage system had been operating for three months; hence, these decreases in groundwater level are related to reservoir drainage.
2. From May 2010 to July 2010, the groundwater level at ZK11 and ZK14 rose by 36.17 and 8.89 m, respectively, because of increased reservoir water level. This was a period of heavy rainfall in the region, which also affected the groundwater level of boreholes ZK11 and ZK14.
3. From December 2010 to March 2011, the groundwater level at ZK11 and ZK14 dropped from 466.14 and 470.37 to 434.67 and 455.23 m, respectively. The decreases in groundwater during this period were induced by reservoir drainage.
4. From April 2011 to July 2011, the groundwater level at ZK11 and ZK14 increased from 428.52 and 453.48 to 454.57 and 461.08 m, respectively. The influence of the heavy rainfall on the groundwater level is more noticeable, because although the water level of the reservoir decreased during this period, the groundwater level increased.

At the upper part of the landslide (borehole ZK2; Fig. 10), three distinct phases can be identified in the groundwater level curve of KZ2, with May 2010 and May 2011 being the demarcation points.

NHESSD
3, 2537–2564, 2015

1. Before May 2010, the groundwater level at ZK2 gradually dropped from 645.49 to 617.91 m. In this period, low rainfall levels led to a decrease in the groundwater level.

2. From May 2010 to May 2011, the groundwater level at ZK2 increased from 617.91 to 647.88 m following heavy rainfall, and then fell to 629.09 m.

3. Since May 2010, the groundwater level at ZK2 increased from 629.09 to 652.21 m because of heavy rainfall, and then fell to 638.40 m.

Overall, as shown in Fig. 10, changes in the reservoir levels mainly affected the groundwater level at the lower part of the landslide, showing *s* positive correlation between the two levels. The permeability of the lower part of the landslide is good. In the upper part of the landslide, the groundwater accumulates because of rainfall; therefore, the permeability of the upper part is poor.

5.2 Deformation and triggering events

Figure 11 shows the monitoring results of displacement over the 2 year recording period between October 2009 and September 2011. The rainfall near the landslide and the reservoir water level are also shown. Taking, for example, the deformation trend of the landside, three stages can be identified.

1. From October 2009 to May 2010 the reservoir water level dropped from 466 to 426 m. The displacements at DLXG02, DLXG03, DLXG05, and DLXG06 (Fig. 11) increased rapidly because of reservoir drainage. The biggest deformation occurred in the lower part of the landslide, after January 2010. There is no significant change in the reservoir water level during this time and the displacements at these four observational points decrease slowly.

2. From May 2010 to March 2011 the reservoir water level rose from 426 to 466 m at first and then dropped from 470 to 428 m. There were many fluctuations in the

reservoir water level during this period and great increases in the displacements of DLXG02, DLXG03, DLXG05, and DLXG06 from May 2010 to July 2010. The biggest displacement increment was about 12.08 mm. From July 2010 to September 2010 the reservoir water level gradually dropped by 6 m, but the deformation of these four observational points decreased by 5.77, 4.10, 2.17, and 4.22 mm, respectively. There were two increases in the displacements of DLXG01, DLXG08, and DLXG09 located in the upper part of the landslide; one occurred after the rainfall events in June 2010 and the other occurred after the rainfall events in September 2010.

3. After March 2011 the displacements of DLXG02, DLXG03, DLXG05, and DLXG06, induced by fluctuations of the reservoir water, increased; the displacements of DLXG01, DLXG08, and DLXG09 increased sharply after rainfall events.

Before this period, the displacement of DLXG04 increased slowly; after April 2011, once the main drainage tunnel was completed, the displacement of DLXG04 decreased by 7.32 mm in May 2011 and rapidly increased after May 2011.

5.3 Movement tendency

With geological investigation and monitored data, it is found that movement of the Donglingxin landslide can be divided into two phases:

1. Creep deformation: before April 2010, as shown in Fig. 11. The rate of this creep movement of landslide was increased slowly and gradually with a movement rate of 0.72–2.12 mm month^{-1}.

2. Instantaneous deformation: roughly since April 2010. The execution of work and inundation were the two principal triggers which activated the landslide, furthermore, rainfall induced the shallow rotational slide.

NHESSD
3, 2537–2564, 2015

6 Stability analysis

The movement of the Donglingxin landslide can be attributed to the strength drop of the sliding zone caused by the increase of pore water pressure, the shear strength of the sliding zone, characterized by the cohesion c and the friction angle φ are given in Table 1 (provided by HydroChina Zhongnan Engineering). The shear strength decreased from 23 kPa and 29.4° for the natural state to 20 kPa and 28° for saturated state.

Three representative engineering profiles: preflies I-I′, II-II′, and III-III′ (Fig. 5) were selected for stability analysis by modified Janbu method under three different conditions: a natural state, a rainfall and an inundation with rainfall. The safety factors of two sliding surfaces were calculated, as given in Table 2.

From Table 2, it is interesting to find that, rainfall had a great negative influence on the stability of the shallow sliding surface, but a minor influence on the stability of the deep sliding surface. Inundation was the opposite, had a great negative influence on the stability of the deep sliding surface.

7 Disaster prediction

The consequence of numerical simulation by YADE (Fig. 12) shows that once the Donglingxin landslide fails, stones and soil with the total debris volume reaching several millions and waves surging to a height of about 34 m. the upriver water level will be rised to 478–490 m by river blocking up in the Qingshui river, the affected area is about 23 km range. Consequently, the Liuchuan town which is 1.5 km away from the landslide with 22 434 inhabitants will be destoryed by surge. 14 km away from the landslide, a small hydropower station with 486 m in elevation will be submerged. The Jianhe county town with 44 057 inhabitants and 476.6 m in elevation is 20 km away from the landslide, it will also be submerged.

NHESSD
3, 2537–2564, 2015

8 Conclusions

Based on monitoring measurements over a period of about 2 years and stability assessment we conclude the following.

1. The geological investigation indicated that the Donglingxin landslide is a large-scale ancient landslide, which is an accumulation of several consequent slides along the bank slope, the slope may appear bedding landslide, and the deformation characteristics shows that the landslide belongs to thrust load caused landslide.

2. Because the accumulated layer landslide is rich in broken stone and gravel, it has good permeability, the rainfall water and reservoir water are prone to permeate through this stratum into the depth of the slope. Thus, they have effect on the strength reduction of the landslide.

3. Due to the narrow valley at the landslide location, the supports and protections measure is difficult to be used, but the movement near the drainage tunnel may be more active after a few months of drainage.

4. Movement of the lower part of the Donglingxin landslide corresponds to water level changes in the Sanbanxi reservoir. The changes are more evident when the reservoir water level rises. Movement of the upper part of Donglingxin landslide corresponds to rainfall events. The movement is greater during and after the wet season.

5. The groundwater level at the lower part of the Donglingxin landslide correlates well with the reservoir water level. The groundwater at the upper part of the Donglingxin landslide corresponds to rainfall events.

6. Stability assessment indicate that the rainfall had a great negative influence on the stability of the shallow sliding surface, but a minor influence on the stability of

NHESSD
3, 2537–2564, 2015
Movement of the Donglingxin landslide, China
J. Yu et al.

the deep sliding surface. The inundation was the opposite, had a great negative influence on the stability of the deep sliding surface.

7. Once the Donglingxin landslide occurrs, the affected area which will be submerged is about 23 km range.

Acknowledgements. This work is financially supported by National Key Technology Research and Development Program (Grant No. 2013BAB06B01), and the National Natural Science Foundation of China (Grant no. 51209075, 51479049,51409082), and the Fundamental Research Funds for the Central Universities (Grant no. 2014B17714).

References

Bai, S., Wang, J., Thiebes, B., Cheng, C., and Yang, Y.: Analysis of the relationship of landslide occurrence with rainfall: a case study of Wudu County, China, Arabian J. Geosci., 7, 1277–1285, 2014.

Fleming, R. W., Ellen, S. D., and Algus, M. A.: Transformation of dilative and contractive landslide debris into debris flows-an example from Marin County, California, Eng. Geol., 27, 201–223, doi:10.1016/0013-7952(89)90034-3, 1989.

Huang, R. Q.: Some catastrophic landslides since the twentieth century in the southwest of China, Landslides, 6, 69–81, 2009.

Iverson, R. M., Reid, M. E., and LaHusen, R.: Debris-flow mobilization from landslides, Annu. Rev. Earth Pl. Sc., 25, 85–138, 1997.

Jin, D. L. and Wang, G. F.: Tangyanguang Landslide in Zhaxi Reservoir, Hunan Province, China, Typical Landslides Occurred in China, Science press, Beijing, 301–307, 1988 (in Chinese).

Qi, S., Yan, F., Wang, S., and Xu, R.: Characteristics, mechanism and development tendency of deformation of Maoping landslide after commission of Geheyan reservoir on the Qingjiang River, Hubei Province, China, Eng. Geol., 86, 37–57, 2006.

Wang, F., Zhang, Y., Huo, Z., Matsumoto, T., and Huang, B.-L.: The July 14, 2003 Qianjiangping landslide, Three Gorges Reservoir, China, Landslides, 1, 157–162, 2004.

Wang, F., Zhang, Y., Huo, Z., Peng, X., Araiba, K., and Wang, G.: Movement of the Shuping landslide in the first four years after the initial impoundment of the Three Gorges Dam Reservoir, China, Landslides, 6, 321–329, 2008.

NHESSD

3, 2537–2564, 2015

Wang, R., Xu, W., and Zhang, J.: Comprehensive assessment and sliding mechanism analysis of Zhenggang Landslide, Southwestern China, Disaster Advances, 5, 327–331, 2012.

NHESSD
3, 2537–2564, 2015

NHESSD
3, 2537–2564, 2015

Movement of the Donglingxin landslide, China

J. Yu et al.

Table 1. Stratigraphic physical and mechanical parameters.

	Strata	Triaxial shear strength c (kPa) Natural	Saturated	φ (°) Natural	Saturated	Density ($g\,cm^{-3}$) Natural	Saturated
Q_4^{del}	i. Coarse-grained silty clay with mixture of broken stones	20	18	26	24	2.0	2.1
	ii. Broken stones and gravel with mixture of silty clay	20	15	35	30	2.15	2.22
	iv. Sliding zone	23	20	29.4	28	2.03	2.08

Table 2. Results of stability analysis with modified Janbu method.

Profile	Sliding surface	Natural	rainfall	Inundation with rainfall
I-I′	shallow	1.133	1.085	1.014
	deep	1.155	1.105	1.023
II-II′	shallow	1.140	1.077	0.995
	deep	1.170	1.132	1.035
III-III′	shallow	1.172	1.127	1.028
	deep	1.209	1.118	1.045

NHESSD
3, 2537–2564, 2015

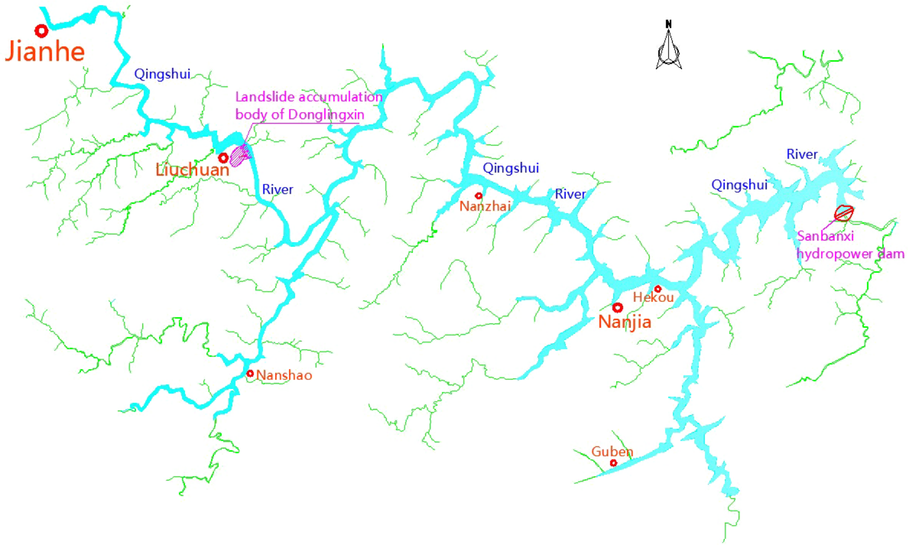

Figure 1. Location map of the Sanbanxi dam and the Donglingxin landslide, China.

NHESSD
3, 2537–2564, 2015

Figure 2. The Donglingxin landslide facing the Qingshui River (taken form Google earth).

NHESSD
3, 2537–2564, 2015

Figure 3. Photo of local village and farmland.

NHESSD
3, 2537–2564, 2015

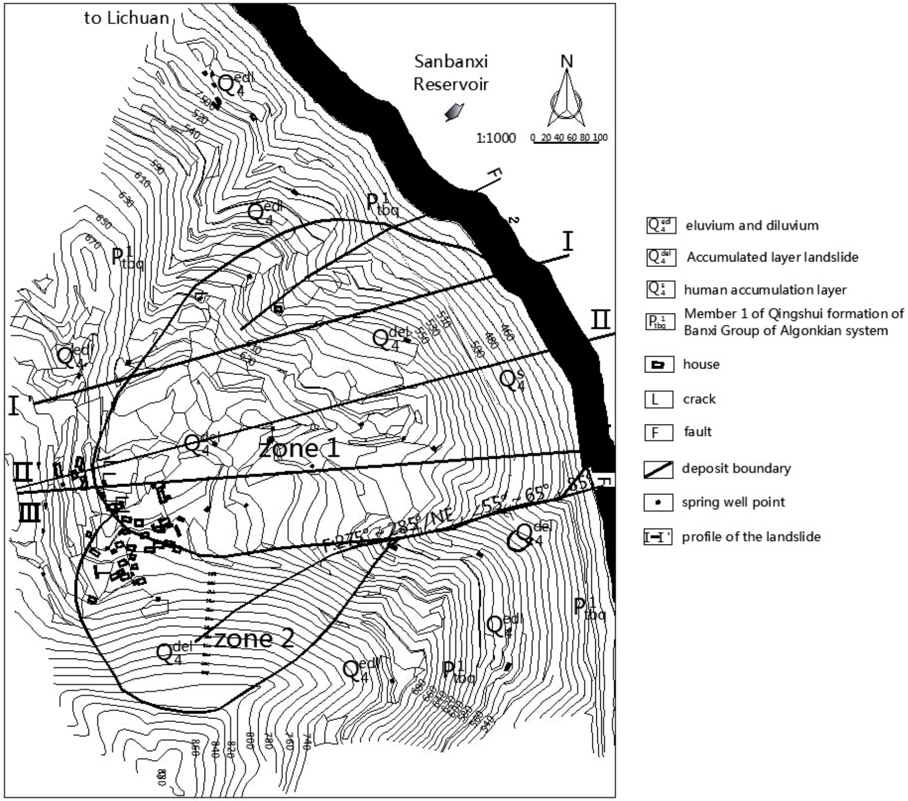

Figure 4. Topography and monitoring locations of the Donglingxin landslide.

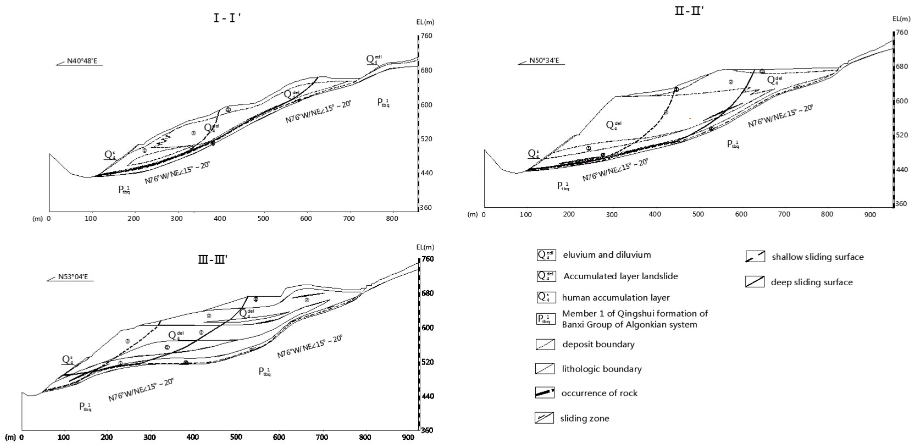

Figure 5. Geological profile of the landslide deposit.

Figure 6. Photo of cracks in farmland at elevation 692 m.

NHESSD

3, 2537–2564, 2015

Figure 7. The phenomenon of muddy water coming from the landslide.

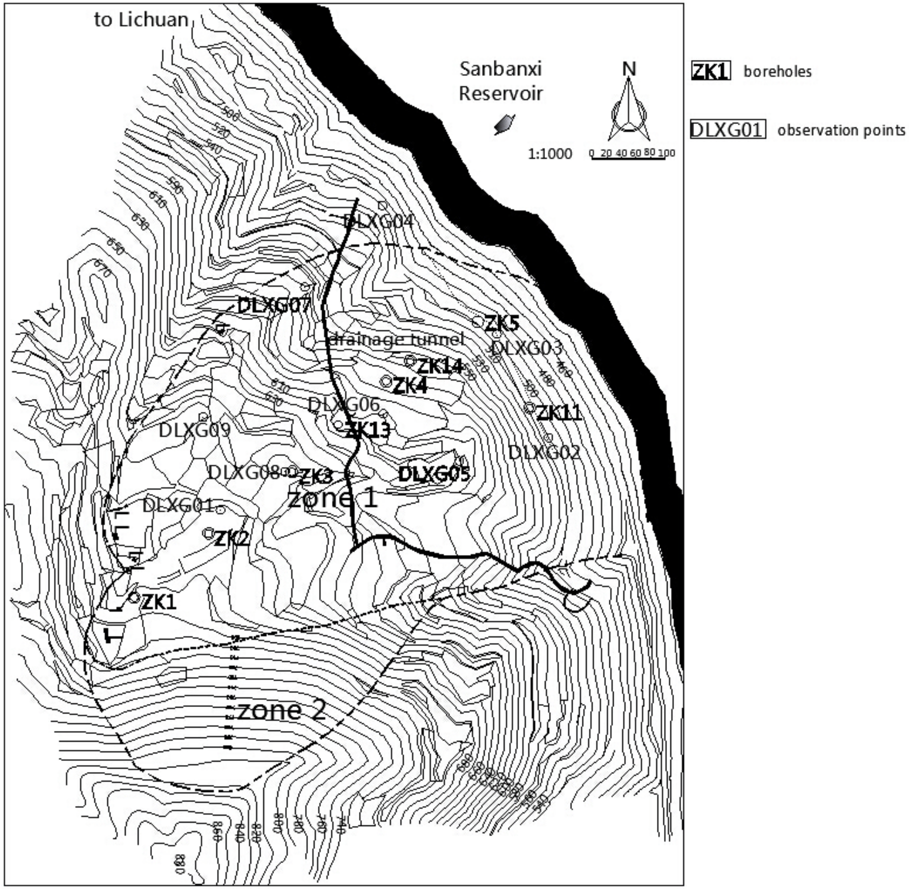

Figure 8. Location of the observation points in the Donglingxin landslide.

NHESSD
3, 2537–2564, 2015

Movement of the Donglingxin landslide, China

J. Yu et al.

Title Page
Abstract Introduction
Conclusions References
Tables Figures
◂◂ ▸▸
◂ ▸
Back Close
Full Screen / Esc
Printer-friendly Version
Interactive Discussion

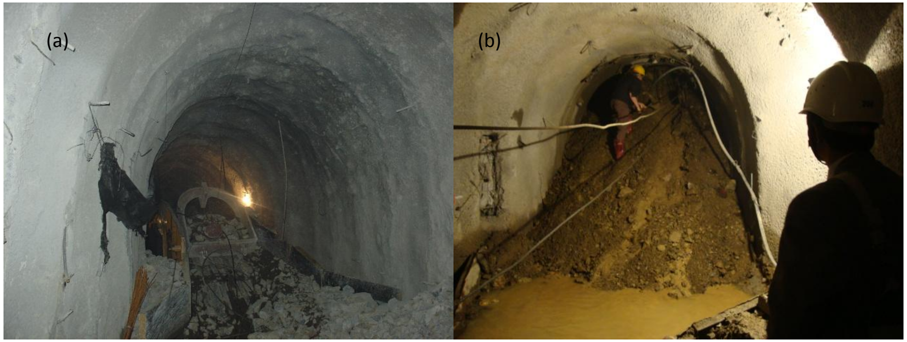

Figure 9. Construction of drainage tunnel EL 500.

NHESSD
3, 2537–2564, 2015

Movement of the Donglingxin landslide, China

J. Yu et al.

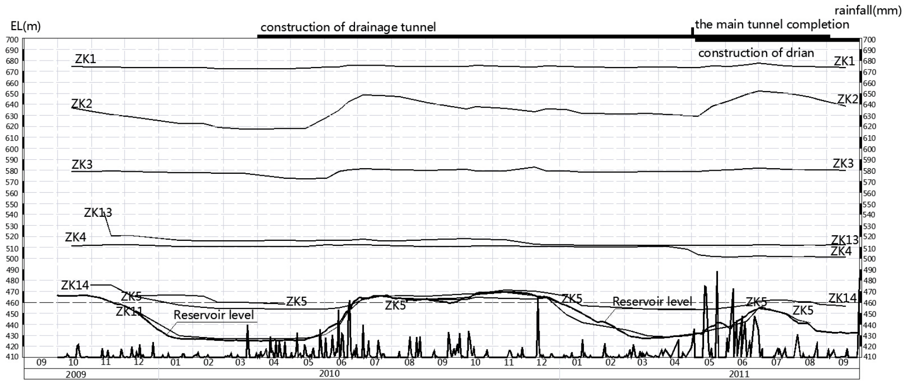

Figure 10. Monitoring results of groundwater levels at boreholes ZK1–ZK5, ZK11, ZK13, and ZK14 for the period October 2009 to September 2011 in the Donglingxin landslide. Rainfall for this period and water level in the Sanbanxi reservoir are also shown.

NHESSD
3, 2537–2564, 2015

Movement of the Donglingxin landslide, China

J. Yu et al.

Title Page
Abstract Introduction
Conclusions References
Tables Figures
Back Close
Full Screen / Esc
Printer-friendly Version
Interactive Discussion

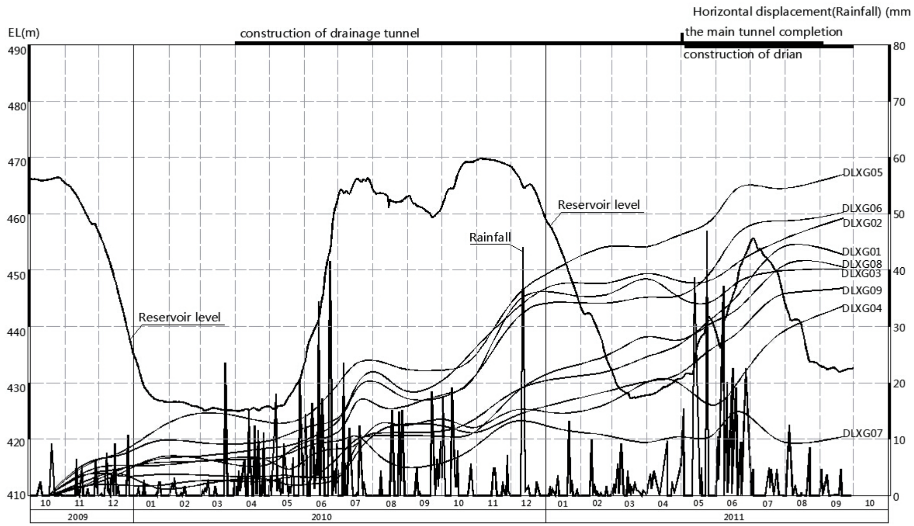

Figure 11. Monitoring results of displacements for the period from October 2009 to September 2011 in the Donglingxin landslide. Rainfall for this period and the water level in the Sanbanxi Reservoir are also shown.

NHESSD
3, 2537–2564, 2015

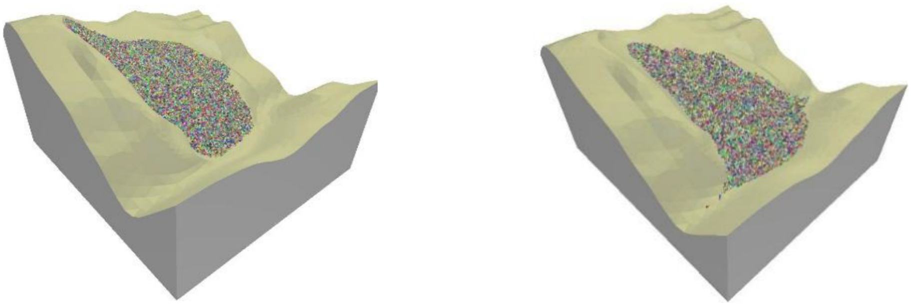

Figure 12. The consequence of numerical simulation by YADE.

NHESSD
3, 2537–2564, 2015